ELSEVIER

Variability in Leaf and Litter Optical Properties: Implications for BRDF Model Inversions Using AVHRR, MODIS, and MISR

Gregory P. Asner, Carol A. Wessman,* David S. Schimel,† and Steve Archer‡*

Canopy radiative transfer models simulate the bidirectional reflectance distribution function (BRDF) of vegetation covers with differing leaf and soil spectral and canopy structural characteristics. Numerical inversion of these models has provided estimates of vegetation structural and biophysical characteristics from multiangle, remotely sensed optical data. The number of angularly unique observations compared to BRDF model parameters largely determines the accuracy of retrievals. To increase this ratio, additional observations of a target must be acquired and the BRDF models and inversions must be simplified. The former will occur when the EOS instruments become available. Previous studies suggest that simplification of BRDF model inversions may best be accomplished by constraining the leaf optical parameters. This study focused on full-range (400–2500 nm) leaf and litter spectral properties convolved to AVHRR, MODIS, and MISR optical channels. Using a diverse array of woody plant and grass species, we found robust and readily usable interrelationships among spectra through correlation, regression, and principal components analyses. Significant differences between green leaf and litter optical properties and their sensor-specific interrelationships indicate that green leaf optical constraints may be useful with BRDF retrievals to detect the onset of canopy senescence. These findings will provide increased efficiency in canopy BRDF model inversions by decreasing the number of observations required to retrieve canopy structural and biophysical information from multiangle remotely sensed data.

INTRODUCTION

The spectral and angular dependence of photons reflected off a surface is governed by the bidirectional reflectance distribution function (BRDF). In the specific case of vegetation canopies, this reflectance distribution is anisotropic and primarily a function of leaf optical properties, canopy architecture, soil surface attributes, illumination conditions, and viewing geometry (Ross, 1981; Goel, 1988; Shultis and Myneni, 1988; Myneni et al., 1988; Jacquemoud et al., 1992). The spectral attributes of a plant canopy are linked to scattering processes at the leaf level. Leaf-level scattering varies with leaf structure, water content, and the concentration of carbon constituents (e.g., lignin, cellulose, starch), chlorophyll, and nitrogen (Gates et al., 1965; Thomas et al., 1971; Wooley, 1971; Walter-Shea and Norman, 1991; Fourty et al., 1996; Jacquemoud et al., 1996). Although the angular variation of scattered photons at the canopy level is tied to leaf and soil spectral properties, it is highly dependent on canopy structural characteristics such as leaf area index and leaf angle distribution (Goel, 1988; Myneni and Asrar, 1993).

Plant canopy radiative transfer (RT) models have advanced from simple light extinction algorithms to those based explicitly on scattering theory using turbid medium and turbid-medium/geometric-optical methods (e.g., Goel, 1988; Myneni et al., 1989; Li et al., 1995). Since these models are based on scattering processes, they provide a valuable tool for quantifying the light regime within canopies and for simulating the scattering of photons from

* Center for the Study of Earth from Space/CIRES and Department of Environmental, Population and Organismic Biology, University of Colorado, Boulder

† National Center for Atmospheric Research, Boulder

‡ Department of Rangeland Ecology and Management, Texas A&M University, College Station

Address correspondence to G. P. Asner CIRES/CSES, Campus Box 216, University of Colorado, Boulder, CO 80309-0216.

Received 19 January 1997; revised 22 August 1997.

REMOTE SENS. ENVIRON. 63:243–257 (1998)

655 Avenue of the Americas, New York, NY 10010

0034–4257/98/$19.00
PII S0034–4257(97)00138–7

a canopy to a remote sensing instrument. In the most generic RT modeling sense, the radiation received by a sensor (R) at any given optical wavelength (λ) can be summarized:

$$R_{\lambda,i}=f(\text{SKY},\text{FOV},\theta_{s(i)},\varphi_{s(i)},\theta_{v(i)},\varphi_{v(i)},P), \quad (1)$$

where

$$\text{P}=\{\text{LAI},\text{LAD},\rho_\lambda(\text{leaf}),\tau_\lambda(\text{leaf}),\rho_\lambda(\text{soil})\}.$$

SKY represents the atmospheric conditions at the time of image acquisition, and FOV is the instantaneous field-of-view of the remote sensing instrument. Sun location during a particular observation (i) is described by a zenith and azimuth angle ($\theta_{s(i)}$, $\varphi_{s(i)}$), and the sensor viewing orientation is given by $\theta_{v(i)}$ and $\varphi_{v(i)}$. P represents a set of tissue (e.g., leaf, stem) optical and canopy structural characteristics. Modeled canopy structural attributes typically include leaf area index (LAI) and leaf angle distribution (LAD). Scattering processes are simulated using measured or modeled leaf reflectance and transmittance [ρ_λ(leaf) and τ_λ(leaf)] and soil reflectance [ρ_λ(soil)] properties (e.g., Marshak, 1989; Jacquemoud et al., 1992).

Using remotely sensed data to sample the angular variation in the canopy BRDF, radiative transfer models can be inverted to estimate vegetation structural and biophysical characteristics such as LAI and the fraction of absorbed photosynthetically active radiation (*f*APAR) (e.g., Goel and Thompson, 1984; Privette et al., 1994; Braswell et al., 1996; Privette et al., 1996). Inversion of a canopy RT model is usually achieved numerically by minimizing the difference between measured BRDF samples (e.g., satellite observations) and modeled canopy reflectance values (Goel, 1988). An optimization routine minimizes a figure-of-merit function that represents this difference between measured and modeled reflectances (Fig. 1). The modeled leaf, soil, and canopy properties leading to the successful minimization of the merit function are the retrieved parameters.

No remote sensing instrument will provide a complete sampling of a surface BRDF, and previous studies have highlighted the general lack of available satellite observations for efficient model inversions (Goel, 1988; Privette et al., 1994; Braswell et al., 1996). Part of the problem rests in obtaining an adequate number of satellite observations with sufficiently unique Sun-view angles ($\theta_{s(i)},\varphi_{s(i)},\theta_{v(i)},\varphi_{v(i)}$) to allow for the most accurate retrievals. Given a limited sampling of the canopy BRDF and potential correlations between spectral bands, only a few degrees of freedom tend to be available in satellite data. The minimum number of angularly unique observations (i) necessary for a retrieval also depends on the number of unconstrained parameters in the BRDF model. These limitations can be summarized in the ratio:

$$[r\cdot i]-1:P_{free}, \quad (2)$$

where r is the number of uncorrelated spectral bands in the ensemble of observations and P_{free} is the number of unconstrained canopy RT model parameters. Note that this ratio alone does not determine the success or failure of an inversion, as there is a strong dependence on other factors such as model parameter sensitivity and the inversion technique itself. Nonetheless, an inversion is not possible without a balanced ratio in Eq. (2).

It is useful to constrain as many variables (P) that are not of interest as possible, either to decrease the minimum number of observations required for an inversion [left side of Eq. (2)] or to increase the ratio of unique observations to unconstrained variables as a safeguard against erroneous retrievals resulting from parameter codependence (Privette et al., 1994). Conversely, constraint of model parameters can decrease the applicability of the BRDF inversion method to new environments which is one of the primary advantages of this physically based method over empirical techniques (e.g., vegetation indices). BRDF parameter constraint can be achieved in two ways: 1) by specifying a possible range of values for a variable through theory and field measurements, and 2) by finding relationships between variables that force them to systematically covary during the model inversion.

Retrieval of canopy structural (e.g., LAI) and biophysical (e.g., *f*APAR) characteristics via BRDF model inversions represents a major step in remote sensing of terrestrial vegetation, with subsequent benefits for biosphere-atmosphere and biogeochemical modeling efforts (Asner et al., 1998; Wessman and Asner, in press). To realize these goals, we seek ways in which canopy RT model parameters might be constrained or linked to improve the retrieval of the most needed canopy information (e.g., *f*APAR, LAI; Running et al., 1994; Field et al., 1995; Asner et al., 1998). We argue that, until future sensors become available for acquiring many samples (i) of the canopy BRDF, practical limitations will require us to choose between parameters of interest. Since canopy-level parameters (e.g., LAI and *f*APAR) are often of primary interest to remote sensing scientists, biosphere–atmosphere modelers, and ecologists, leaf optical properties tend not to be a direct goal of retrievals. This, of course, does not hold true in efforts to retrieve canopy chemical characteristics from remotely sensed hyperspectral data (e.g., Wessman et al., 1988; Jacquemoud et al., 1996). However, current and planned off-nadir looking instruments employable for BRDF inversion methods do not have the high spectral resolution necessary for canopy chemistry estimates. Since LAI and LAD are extremely heterogeneous within and among species in both space and time, leaf optical properties are the best candidates for constraint in BRDF model inversions.

The NOAA Advanced Very High Resolution Radiometer (AVHRR) is currently one of the few spaceborne instruments capable of acquiring off-nadir radiance measurements with adequate repeatability for BRDF model inversions (Barnsley et al., 1994). With two uncorrelated

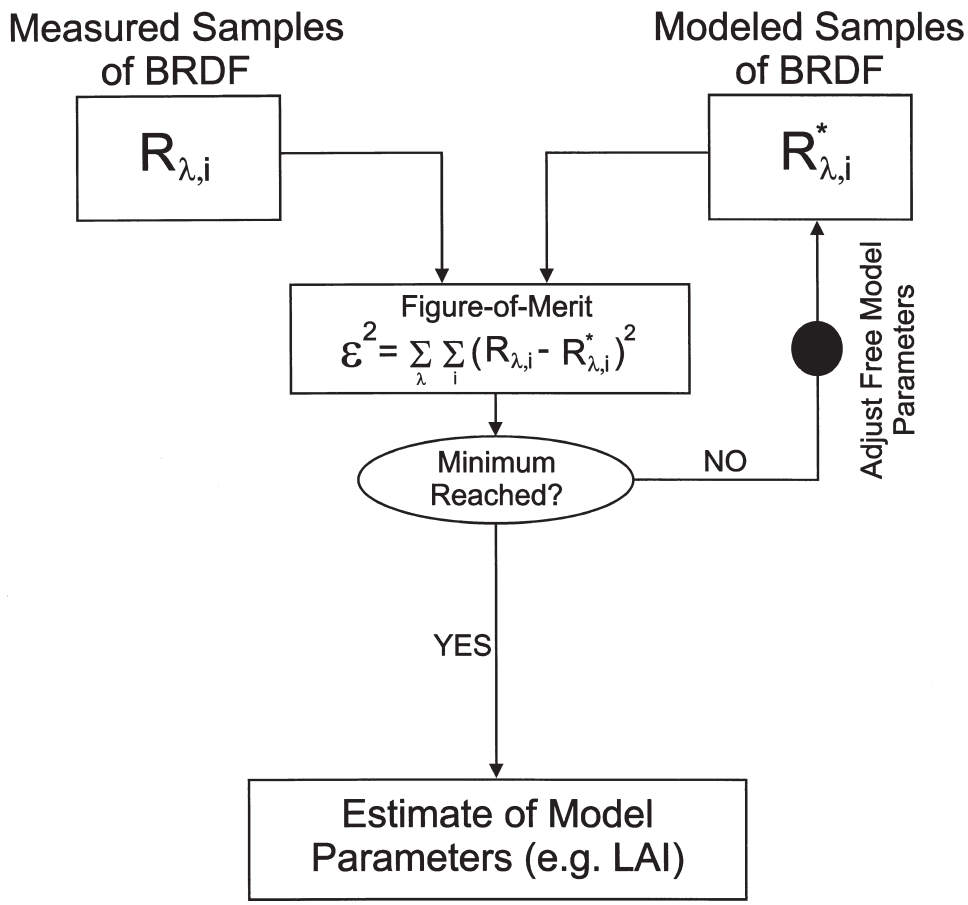

Figure 1. The BRDF model inversion process: A figure-of-merit function (example given) lies at the core of the inversion technique. It is used to minimize the difference between satellite or aircraft measurements of the canopy BRDF and model output generated using the same optical wavelengths and Sun-view geometries. All unconstrained model parameters are adjusted in an iterative manner until the difference between measured and modeled reflectance values is minimized. The parameters leading to the successful minimization of the merit function are then considered "retrieved."

optical channels (one visible, one near-IR) for vegetation, four leaf optical property parameters (two reflectance, two transmittance) are required to take full advantage of a canopy BRDF model using AVHRR data. Braswell et al. (1996) recently linked three leaf optical parameters convolved to the AVHRR Channels 1 and 2 (NIR reflectance, VIS and NIR transmittance) to VIS reflectance using a principal components analysis, and thus decreased the critical number of observations (i) required for a successful model inversion. However, the leaf optical property interrelationships observed by Braswell et al. (1996) were derived from a study of only a few plants grown in greenhouse (water and fertilizer) conditions, and thus the general applicability of these relationships remains unknown.

The Moderate Resolution Imaging Spectrometer (MODIS) and the Multi-angle Imaging Spectroradiometer (MISR), to be launched on the EOS AM-1 platform in 1998, will also provide an off-nadir imaging capability. These instruments will have a spectral resolution superior to that of the AVHRR, with 20 optical channels for MODIS and four for MISR. Provided with seven land surface MODIS bands (Channels 1–7) or four MISR bands, the potential exists for 14 and 8 free leaf-level optical parameters (1 refl. and 1 trans. value per optical channel), respectively. These, in addition to canopy parameters such as LAI and LAD, would result in a very large model parameter set [P in Eq. (2)], making an inversion using all optical channels very difficult.

Leaf spectral properties and their interrelationships over the full optical range (400–2500 nm) have not been well quantified for a wide range of species under field conditions. Even less is known of the variability across environmental gradients. These shortcomings significantly limit canopy BRDF model inversion efforts. Based on the demonstrated need for reducing the number of satellite observations required for accurate and efficient canopy BRDF inversions, we initiated this study to increase our understanding of the variability and interrela-

Table 1. Tree, Shrub, and Grass Foliage Samples Collected along a Climatic Gradient Extending from Northern to Southern Texas

Site Name	*Resource Area*[1]	*Location (latitude)*	*Annual PPT (mm)*	*MAT (°C)*	*Growing Season (d)*	*Woody Cover (%)*	*Dominant Vegetation*
Vernon[2]	Rolling Plains	33°57′N	620	17	220	10–30	*Prosopis glandulosa* savanna grassland
Sonora[3]	Edwards Plateau	30°10′N	575	20	240	10–30	*Quercus-Juniperus* savanna parkland
La Copita[4]	Rio Grande Plains	27°40′N	680	22	290	30–70	*Prosopis-Acacia* savanna parkland

PPT=precipitation; MAT=mean annual temperature. For detailed summaries of climate, soils, and vegetation see: [1]McMahon et al. (1984), [2]Heitschmidt et al. (1986), [3]Amos and Gehlbach (1988), and [4]Archer (1995).

tionships among leaf optical properties across a wide range of plant species, genera, lifeforms, growthforms, and functional groups along a pronounced climate gradient. We also analyzed the optical properties of standing litter tissue because of its significant contribution to ground cover in grasslands, savannas, shrublands, and woodlands. Our specific objectives were: 1) Quantify the variability in leaf and litter full-range (400–2500 nm) optical properties across a diverse array of tree, shrub, and herbaceous species; (2) explore the relationships among leaf and litter optical properties in AVHRR optical channels for potential constraint in canopy BRDF inversions; and (3) document interrelationships among leaf optical properties in MODIS and MISR optical channels.

METHODS

Field Data Collection

Leaf spectral measurements were obtained from three savanna ecosystems that occur along a 900 km north–south climatic gradient in Texas, USA from October 20 to 30 1996 (Table 1). Each of these savanna sites contained a spatially heterogeneous mix of grasses and woody plants. Many of the genera sampled also occur in savannas, shrublands, grasslands, and woodlands of South America, Africa, and Australia. The woody species sampled were from diverse taxonomic families and represented plant functional groups which varied in stature (arborescents to subshrubs), leaf longevity (evergreen to deciduous), leaf texture/thickness (malacophyllous to coriacous to sclerophyllous), pubescence, and leaf nitrogen content (>3% for some leguminous shrubs; <1% for evergreen sclerophylls). The dominant grasses across the three sites were of the C_4 photosynthetic pathway, but some locally abundant C_3 grasses were also sampled for comparison. Plant nomenclature follows Hatch et al. (1990).

For woody species, 5–10 branches (each containing many leaves) were clipped from sunlit positions of mature plants, placed in airtight polyethylene bags, and stored in a cooler. For grasses, whole clumps (including some roots and soil) were removed and stored in airtight bags to maintain leaf moisture. All measurements on woody and grass leaves were conducted within 15 min of sample collection in the field.

Hemispherical reflectance and transmittance values (400–2500 nm) were obtained using a field spectroradiometer (FieldSpec FR, Analytical Spectral Devices, Inc., Boulder, Colorado), a $BaSO_4$ integrating sphere (Licor-1800, Licor, Lincoln, Nebraska), and a modified light source for full spectral range measurements. The spectroradiometer acquires radiance measurements in 1.4 nm intervals within the visible/NIR spectral range and 2 nm intervals in the shortwave IR (SWIR) region. Each leaf reflectance and transmittance measurement was comprised of a 200 spectrum average. A modified version of the Daughtry et al. (1989) method for spectral analyses of conifer needles was used for the grasses and leaflets of woody species (e.g., *Acacia* and *Prosopis*) that did not completely cover the sample port on the integrating sphere. We also used the approach of Middleton et al. (1996) and Mesarch et al. (in review) to decrease the gap fraction between leaf samples in the sample port to less than 20%, and thus minimize errors in transmittance measurements. Only the adaxial surfaces of all leaf and litter samples were measured.

Variability in Leaf and Litter Hyperspectral Data

Analysis of the variability in leaf optical properties across the 400–2500 nm spectral range was first conducted to determine potential differences between plant species, genera, lifeform, growthform, and functional groups. A total of 335 samples from 38 different tree, shrub, and grass species were compared. The mean and standard deviation of the adaxial reflectance and transmittance values within a vegetation type was compared with the woody plant and grass group averages using standard *t*-tests at each wavelength.

AVHRR Channel 1 and 2 Relationships

Leaf and standing litter spectral measurements were convolved to the AVHRR Channel 1 (visible) and 2 (near-IR) spectral response curves as follows:

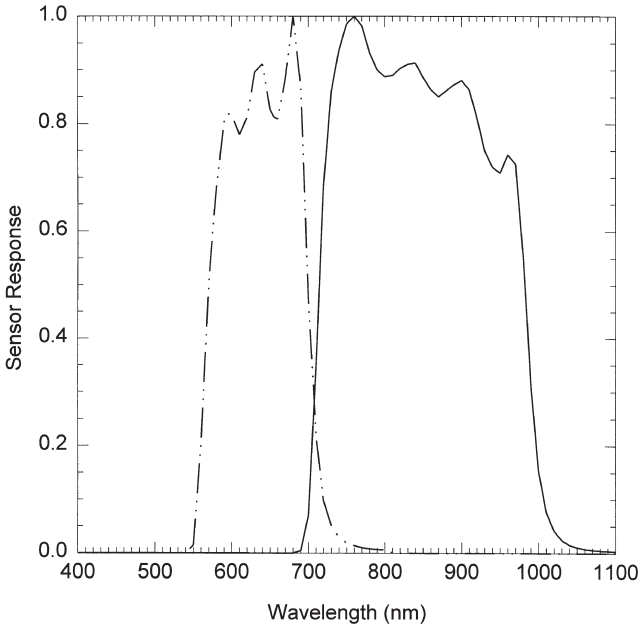

Figure 2. AVHRR Channel 1 (visible) and Channel 2 (NIR) spectral response functions. Channel 1 is shown with a dash-dot line, and Channel 2 is shown with a solid line.

$$\rho_q = \frac{\int_\lambda \rho(\lambda) \cdot S_q(\lambda)}{\int_\lambda S_q(\lambda)}, \quad (3)$$

where q is the sensor channel and S is the response weight at wavelength λ (Fig. 2).

Pearson Product Moment correlation and least squares regression analyses were used to reveal potential relationships between Channel 1 and 2 adaxial reflectance and transmittance values. A principal components analysis (PCA) was then used to determine if leaf and litter reflectance and transmittance values in Channels 1 and 2 (four parameters total) could be represented with fewer than all four parameters in a canopy BRDF model.

MODIS and MISR Optical Channels

Actual MODIS and MISR spectral response curves were not available at the time of this study. However, a Gaussian function was used to extend the leaf and litter optical properties analysis to MODIS and MISR optical channels. Published band centers and widths (Ardanuy et al., 1991) were used to compute a Gaussian function for each channel:

$$f(\lambda) = \exp\left(-(c-\lambda)^{2 \cdot FWHM}\right), \quad (4)$$

where c is the center wavelength for a particular channel. The full width of the Gaussian function at half-maximum was calculated as

$$FWHM = \frac{1.665}{w} \quad (5)$$

Table 2. MODIS and MISR Optical Channels, Band Centers, and Bandwidths Used to Convolve Leaf and Litter Reflectance and Transmittance Measurements

Instrument	*Channel*	*Center Wavelength (nm)*	*Bandwidth (nm)*
MODIS	1	645	50
	2	859	35
	3	469	20
	4	555	20
	5	1240	20
	6	1640	24
	7	2130	50
MISR	1	443	35
	2	555	20
	3	670	15
	4	865	40

and the bounds of the function were determined using

$$b_u = c + (1.5 \cdot w)$$
$$b_l = c - (1.5 \cdot w) \quad (6)$$

where b_u *and* b_l represent the truncated upper and lower bounds of the Gaussian function and w is the published band width.

Since MODIS Channels 8–20 are highly correlated to Bands 1–7 for vegetation targets, all analyses were limited to the first seven channels (Table 2). These channels are already considered the primary land application spectral bands (Ardanuy et al., 1991; Running et al., 1994). Following the band convolution for each MODIS channel, mean reflectance and transmittance values and correlation matrices of the leaf and litter spectra were calculated. A principal components analysis was then used to assess the feasibility of allowing leaf optical properties to covary with one or a few free leaf parameters. MISR Channels 1–4 were also modeled with the Gaussian function [Eqs. (4)–(6); Table 2], and the correlation and PCA tests were conducted.

RESULTS AND DISCUSSION

Leaf and Litter Hyperspectral Variability

We were unable to find any consistent trends or differences in leaf optical characteristics by species, genera, growthforms (e.g., trees vs. shrubs), or functional groups (e.g., nitrogen-fixing vs. nonfixing) (t-tests at each wavelength). There were many differences between woody plant species at various wavelengths, but these differences were inconsistent even among samples within a single species. The variability within genera, growthform, and functional groups always exceeded that of any single species, but no single species was significantly different from these groupings (t-tests by wavelength). Species representing the woody growthforms were subsequently pooled for further analyses. Likewise, there were no consistent differences

between species, genera, or by C_3/C_4 physiology within the overall grass group. Again, the variance within any given species tended to be less than that observed by genus or photosynthetic pathway (C_3 vs. C_4), but no general trends or differences could be found.

Mean leaf reflectance of the grass group was significantly higher than that of the woody plant group throughout the visible (400–700 nm) spectral region and consistently lower in the NIR (700–1400 nm) region (*t*-tests, $p<0.05$, Fig. 3a). Reflectance values throughout the SWIR (1400–2500 nm) region were similar between the woody plant and grass groups. Greater variability in the NIR and SWIR regions is indicative of differences in leaf water content, mesophyll structure, and organic chemistry (Verdebout et al., 1994; Gao and Goetz, 1995; Fourty et al., 1996; Jacquemoud et al., 1996). No significant differences in transmittance values between woody plant and grass groups were found (Fig. 3b).

Grass litter optical properties were more variable in comparison to green leaf material (Fig. 4). Standard deviations in both reflectance and transmittance values reached a maximum of 10% (absolute) in the 2000–2400 nm range. Among grass litter samples, the strong absorption features associated with living chlorophyll in the visible region (~450 and 680 nm) are absent, and several SWIR features related to lignin and cellulose content are evident (Fourty et al., 1996). The lower water content in litter relative to fresh leaf material allows these organic chemical features (e.g., lignin at ~2380 nm) to emerge in the spectra (Verdebout et al., 1994; Jacquemoud et al., 1996).

AVHRR Channel 1 and 2 Relationships

Woody plant and grass spectra convolved to AVHRR Channels 1 (VIS) and 2 (NIR) are shown in Table 3. The greatest variability in reflectance and transmittance occurred in the NIR channel. Grasses had higher VIS reflectance and lower NIR reflectance and transmittance values than the woody plant group, although only the VIS reflectance difference was statistically significant (*t*-tests, $p<0.05$). The consistent VIS spectral properties across the wide variety of species examined in this study may be the result of offsetting biophysical properties associated with leaf thickness, chlorophyll concentration, and other factors that interact dynamically to maintain leaf optical properties within narrow ranges. For example, leaves in full sunlight conditions tend to be thicker but have less chlorophyll per unit leaf mass, whereas leaves from shaded portions of the canopy tend to be thinner with higher chlorophyll per unit leaf mass (Poorter et al., 1995). Several studies have demonstrated that strong gradients of light intensity (e.g., vertical location in canopy), leaf mass and thickness, and chlorophyll concentration fail to contribute to significant variation in leaf optical properties at visible wavelengths (Lee and Graham, 1986; Fetcher et al., 1994; Poorter et al., 1995). Our results further suggest that VIS leaf optical properties are dynamically stable along a pronounced climate gradient (Table 1).

Correlation analyses of the entire leaf optical properties data set (woody species+grasses) in AVHRR Channels 1 and 2 revealed three significant relationships (Table 4): 1) NIR reflectance was inversely related to VIS transmittance; 2) NIR reflectance was inversely related to NIR transmittance; and 3) VIS transmittance was positively related to NIR transmittance. There were no significant correlations between VIS reflectance and any other measurement.

Principal components analysis of the mean-corrected data indicated that 90% of the variance in the entire (woody species+grass) data set could be explained by the first PC (Table 5). The eigenvector loading on PC 1 indicated that the contribution of the VIS reflectance measurement (−0.004) was insignificant. This was consistent with the narrow range of VIS reflectance values within and among species (Table 3). PC 2 accounted for 8% of the total variance, and, again, VIS reflectance was insignificant.

Variability of leaf reflectance in AVHRR Channel 1 (VIS) was quite small (Table 3), uncorrelated with the other three measurements (Table 4), and contributed little to the total variance in the data (Table 5). As a result, it can be treated as a constant (~9% for woody species and ~12% for grasses) in canopy RT models. In RT model inversions, VIS reflectance can be constrained to a very narrow range (e.g., 7–11% includes four standard deviations for woody species), reducing the number of totally free leaf optical parameters to three. Furthermore, because VIS and NIR transmittance parameters were highly correlated with each other ($r=0.93$; Table 4) and both were highly correlated with NIR reflectance ($r=-0.78$ and -0.81), the group of four leaf parameters can be reduced to one free parameter: NIR reflectance. Least squares regression analyses between these correlated bands yielded the following relationships:

$$\begin{aligned} \tau_{NIR} &= 0.30 + 1.80(\tau_{VIS}), \quad r^2 = 0.86, \\ \tau_{NIR} &= 0.88 - 1.08(\rho_{NIR}), \quad r^2 = 0.62, \\ \tau_{VIS} &= 0.32 - 0.58(\rho_{NIR}), \quad r^2 = 0.66. \end{aligned} \tag{7}$$

Another approach utilizes the PCA results more directly. Since 90% of the variance in the AVHRR leaf optical data was explained by the first PC, any one parameter can be written in terms of the remaining three using the eigenvectors of PC 1 and the mean-corrected reflectance and transmittance values (Braswell et al., 1996). For example, VIS reflectance (ρ_{VIS}), VIS transmittance (τ_{VIS}), and NIR transmittance (τ_{NIR}) can be approximated in terms of NIR reflectance (ρ_{NIR}) as

$$\rho_{VIS} \approx \frac{e_1}{e_2}\rho_{NIR} + \left(\overline{\rho_{VIS}} - \frac{e_1}{e_2}\overline{\rho_{NIR}}\right),$$

$$\tau_{VIS} \approx \frac{e_3}{e_2}\rho_{NIR} + \left(\overline{\tau_{VIS}} - \frac{e_3}{e_2}\overline{\rho_{NIR}}\right),$$

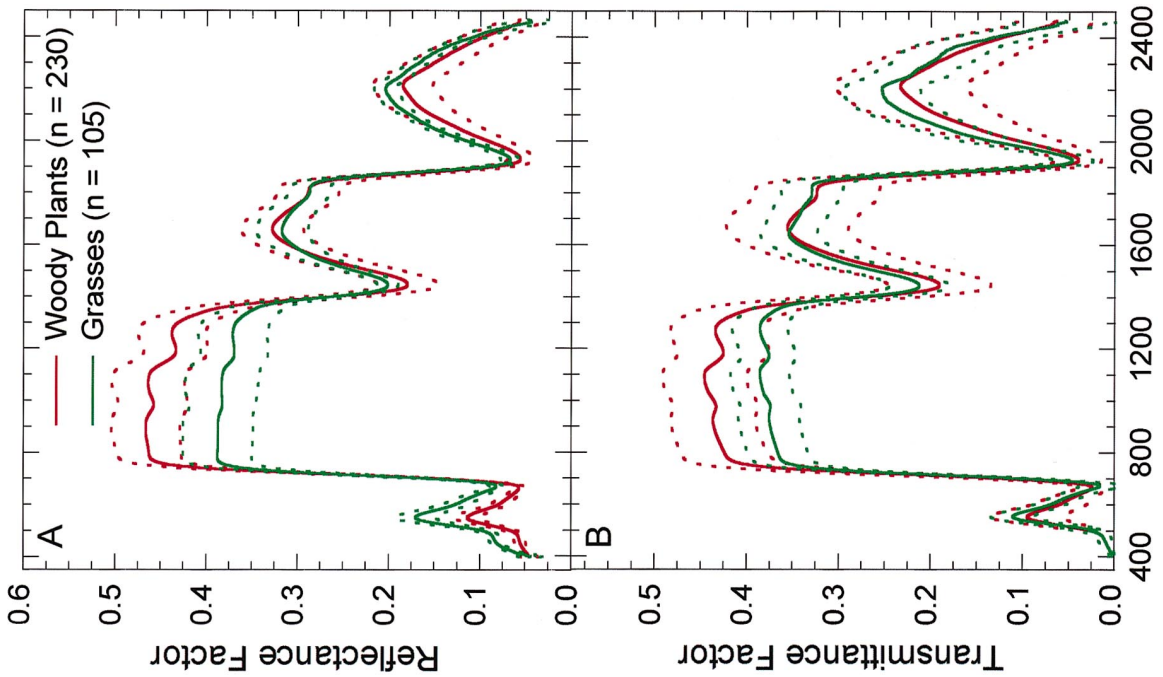

Figure 3. A) Full optical range leaf hemispherical reflectance and B) transmittance spectra for woody plant (red) and grass (green) vegetation groups. Means are shown as solid lines; dotted lines depict ±1 standard deviation.

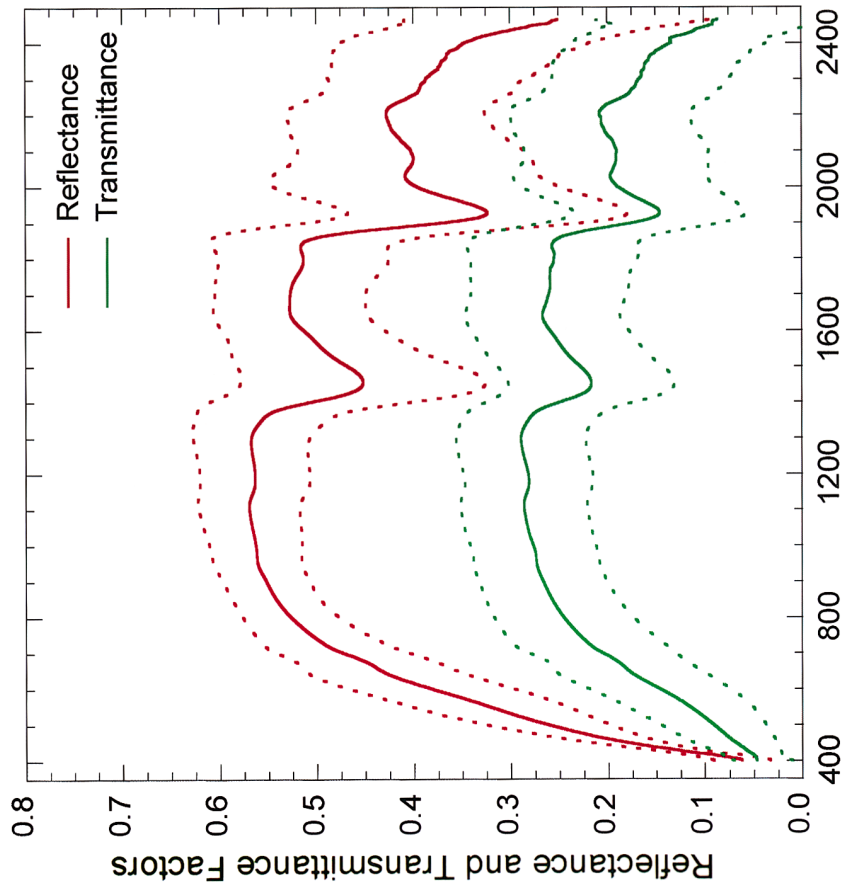

Figure 4. Full optical range grass litter hemispherical reflectance (red) and transmittance (green) spectra. Means are shown as solid lines; dotted lines depict ±1 standard deviation.

Table 3. Variability of Tree, Shrub, and Grass Leaf Optical Properties in AVHRR Channel 1 (VIS) and Channel 2 (NIR)[a]

		Reflectance		*Transmittance*	
Life Form	*Species*	*VIS*	*NIR*	*VIS*	*NIR*
Trees/shrubs	*Acacia berlandieri* (L)*	0.07 (0.00)	0.39 (0.02)	0.03 (0.01)	0.32 (0.04)
	Acacia farnesiana (L)*	0.09 (0.00)	0.41 (0.02)	0.07 (0.02)	0.35 (0.02)
	Acacia greggii (L)	0.08 (0.01)	0.43 (0.04)	0.02 (0.02)	0.31 (0.02)
	Acacia rigidula (L)*	0.08 (0.01)	0.39 (0.04)	0.04 (0.02)	0.36 (0.02)
	Acer negundo	0.10 (0.01)	0.40 (0.02)	0.08 (0.02)	0.44 (0.02)
	Celtis reticulata	0.09 (0.01)	0.46 (0.03)	0.05 (0.02)	0.39 (0.04)
	Cercis canadensis (L)	0.08 (0.01)	0.42 (0.02)	0.08 (0.00)	0.43 (0.01)
	Colubrina texensis	0.09 (0.01)	0.42 (0.01)	0.06 (0.00)	0.43 (0.01)
	Diospyros texana	0.08 (0.01)	0.47 (0.01)	0.04 (0.01)	0.37 (0.02)
	Forestiera angustifolia	0.09 (0.01)	0.48 (0.01)	0.06 (0.01)	0.40 (0.01)
	Leucaena retusa (L)	0.09 (0.01)	0.42 (0.01)	0.08 (0.01)	0.46 (0.01)
	Lonicera albiflora	0.08 (0.00)	0.44 (0.01)	0.08 (0.01)	0.45 (0.01)
	Mahonia trifoliolata (EG-S)	0.09 (0.01)	0.44 (0.02)	0.03 (0.01)	0.31 (0.03)
	Morus microphylla	0.08 (0.01)	0.41 (0.01)	0.07 (0.01)	0.44 (0.00)
	Populus angustifolia	0.09 (0.00)	0.46 (0.01)	0.03 (0.00)	0.34 (0.01)
	Prosopis glandulosa (L)	0.08 (0.00)	0.36 (0.02)	0.06 (0.03)	0.39 (0.03)
	Quercus buckleyi	0.08 (0.01)	0.42 (0.01)	0.08 (0.00)	0.45 (0.01)
	Quercus gambelii	0.08 (0.01)	0.42 (0.01)	0.07 (0.02)	0.40 (0.02)
	Quercus pungens (EG-S)	0.08 (0.00)	0.47 (0.01)	0.05 (0.00)	0.38 (0.01)
	Quercus virginiana (EG-S)	0.09 (0.00)	0.47 (0.01)	0.03 (0.00)	0.33 (0.01)
	Rhus aromatica	0.09 (0.01)	0.43 (0.01)	0.07 (0.01)	0.41 (0.02)
	*Rhus microphylla**	0.10 (0.01)	0.41 (0.02)	0.07 (0.02)	0.35 (0.02)
	Sophora secundiflora (EG-S)	0.09 (0.00)	0.52 (0.02)	0.02 (0.00)	0.32 (0.02)
	Ungnadia speciosa	0.09 (0.01)	0.41 (0.01)	0.12 (0.01)	0.48 (0.01)
	Zanthoxylum fagara (EG-NS)	0.08 (0.01)	0.42 (0.02)	0.06 (0.01)	0.39 (0.08)
	All Trees/Shrubs (n=230)	0.09 (0.01)	0.43 (0.04)	0.06 (0.03)	0.39 (0.06)
Grasses	*Agropyron cristatum* (C3)	0.12 (0.01)	0.42 (0.01)	0.08 (0.02)	0.36 (0.01)
	Aristida purpurea	0.10 (0.00)	0.35 (0.01)	0.05 (0.00)	0.36 (0.01)
	Bothriochloa ischaemum	0.14 (0.01)	0.37 (0.00)	0.06 (0.00)	0.36 (0.00)
	Bouteloua curtipendula	0.12 (0.01)	0.36 (0.02)	0.05 (0.01)	0.38 (0.01)
	*Bouteloua rigidiseta**	0.12 (0.01)	0.37 (0.02)	0.07 (0.01)	0.39 (0.01)
	*Cenchrus ciliaris**	0.10 (0.00)	0.38 (0.00)	0.05 (0.00)	0.40 (0.01)
	Chloris pluriflora	0.12 (0.01)	0.36 (0.02)	0.05 (0.01)	0.39 (0.01)
	*Erioneuron pilsoum**	0.13 (0.01)	0.37 (0.01)	0.06 (0.00)	0.37 (0.00)
	*Hilaria belangeri**	0.11 (0.00)	0.33 (0.02)	0.04 (0.00)	0.31 (0.01)
	Schizachyrium scoparium	0.10 (0.00)	0.35 (0.01)	0.05 (0.00)	0.36 (0.00)
	*Sorghastrum nutans**	0.14 (0.01)	0.38 (0.02)	0.06 (0.02)	0.41 (0.01)
	Stipa leucotricha (C3)	0.12 (0.02)	0.41 (0.01)	0.08 (0.02)	0.37 (0.01)
	Tripsacum dactyloides	0.10 (0.01)	0.40 (0.01)	0.05 (0.00)	0.44 (0.01)
	All Grasses (n=105)	0.12 (0.01)	0.38 (0.03)	0.06 (0.02)	0.37 (0.03)

[a] Means are given with standard deviations in parentheses. n=10 per species unless an asterisk (*) indicates n=5. Plant nomenclature follows Hatch et al. (1990). L=leguminous species; EG-S=evergreen species with sclerophyllous (thick, waxy cuticle) leaves; EG-NS=evergreen species without sclerophyllous leaves. Tree/shrub species without notation are deciduous. C3=grass with C_3 physiology. Grasses without notation have C_4 physiology.

$$\tau_{NIR} \approx \frac{e_4}{e_2}\rho_{NIR} + \left(\overline{\tau_{NIR}} - \frac{e_4}{e_2}\overline{\rho_{NIR}}\right), \quad (8)$$

where the e_i are the weights of the eigenvector associated with the first PC (row 1 of Table 5), and $\overline{\rho}$ and $\overline{\tau}$ are the mean reflectance and transmittance values of the AVHRR-convolved leaf optical data set (Table 3). In effect, this method of collapsing the number of free parameters (P_{free}) could reduce the number of required unique Sun-satellite view observations (i) by three as well [Eq. (2)].

Grass litter spectral properties were highly variable in both AVHRR optical channels (Table 6). Variability within a species was slightly less than that observed for all litter data combined, and no channel was more consistent than another channel. Variable decay rates and microclimate differences result in significantly different spectral properties at virtually all optical wavelengths (Fig. 4).

The correlation matrix of the AVHRR-convolved litter spectra was much different than that obtained for green leaf optical properties (Table 4). Significant correlations occurred between VIS and NIR reflectance (r=0.78) and between VIS and NIR transmittance (r=0.89). A significant but less robust relationship occurred between NIR reflectance and NIR transmittance (r=−0.55). The first

Table 4. Correlation[a] Matrices for Green Leaf (Woody Plant+Grass) and Grass Litter Reflectance and Transmittance Values Convolved to AVHRR Channels 1 (VIS) and 2 (NIR)

	VIS Refl.	*NIR Refl.*	*VIS Tran.*	*NIR Tran.*
Leaf				
VIS Refl.	—	0.06	0.15	−0.0
NIR Refl.		—	−0.81*	−0.78*
VIS Tran.			—	0.93*
NIR Tran.				—
Litter				
VIS Refl.	—	0.78*	0.33	−0.08
NIR Refl.		—	−0.20	−0.55*
VIS Tran.			—	0.89*
NIR Tran.				—

* $P<0.0001$.
[a] Pearson Product Moment Method.

two principal components explained 54% and 44% of the variance, respectively (Table 5). Because all four leaf optical parameters contributed significantly to either PC 1 or PC 2, the PCA method outlined in Eq. (8) would not be accurate for senescent grass canopies.

The fact that green and senescent foliage must be treated differently in BRDF inversions may create retrieval problems when canopies begin to shift from a photosynthetically active to senescent (e.g., with stress or phenology) status. This may, in fact, indicate the possibility of detecting the onset of canopy senescence using BRDF inversion methods. Errors will be most evident early in the shift from live to dead standing biomass before canopy-level structural characteristics (e.g., LAI) change significantly. In canopies comprised of a heterogeneous mix of live and dead leaf tissue (e.g., late season grasslands), only the consistently high correlation between VIS and NIR transmittance remains valid.

MISR and MODIS Leaf Optical Properties

Mean reflectance and transmittance, correlation analyses, and principal components analysis of green leaf spectra convolved to MISR channels are shown in Table 7. We will discuss only those correlations above or below the ± 0.50, $p<0.05$ threshold (bold values in Table 7b) since relationships of lesser strength are unlikely to be directly useful for narrowing the number of free leaf parameters in a BRDF model inversion. Based on this threshold, MISR Bands 1 and 2 (blue and green spectral regions) were each correlated with Band 3 (red), suggesting that additional visible wavelength bands will not increase the observation:free parameter ratio [Eq. (2)] when moving from the AVHRR to MISR. As with the AVHRR bands, the NIR channel (4) was correlated with all transmittance measurements, and the transmittance measurements were highly correlated amongst themselves.

The PCA indicated 99% of the total variance was explained by the first principal component (Table 7c). Bands 1 (blue) and 3 (red) played a very small role (small eigenvector weights) in producing the first PC. Thus, it appears that MISR Bands 2 (green) and 4 (NIR) would be the most suitable (in terms of leaf optical parameters) for use in BRDF inversions. From a spectral resolution perspective, MISR may not provide a significant im-

Table 5. Principal Components Analysis of Green Leaf (Woody Plant+Grass) and Grass Litter Reflectance and Transmittance Properties Convolved to AVHRR Channels 1 (VIS) and 2 (NIR)

		Eigenvectors			
	Eigenvalue	*VIS Refl.*	*NIR Refl.*	*VIS Tran.*	*NIR Tran.*
Fresh leaf					
PC 1	0.90	−0.004	−0.492	0.389	0.779
PC 2	0.08	−0.020	−0.860	−0.080	−0.504
PC 3	0.01	−0.700	−0.082	−0.655	0.271
PC 4	0.01	−0.713	0.108	0.643	−0.257
Standing litter					
PC 1	0.54	−0.170	0.152	−0.721	−0.655
PC 2	0.44	−0.848	−0.468	−0.105	0.225
PC 3	0.01	−0.427	0.871	0.074	0.232
PC 4	0.01	−0.263	−0.005	0.681	−0.683

Table 6. Variability of Grass Litter Optical Properties in AVHRR Channels 1 (VIS) and 2 (NIR)[a]

	Reflectance		*Transmittance*	
Species[b]	*VIS*	*NIR*	*VIS*	*NIR*
Agropyron cristatum (C3)	0.45 (0.04)	0.53 (0.04)	0.12 (0.04)	0.19 (0.04)
Aristida purpurea	0.41 (0.03)	0.50 (0.05)	0.18 (0.05)	0.23 (0.02)
Bothriochloa ischaemum	0.47 (0.03)	0.56 (0.02)	0.13 (0.03)	0.18 (0.03)
Bouteloua curtipendula	0.37 (0.06)	0.51 (0.04)	0.10 (0.04)	0.18 (0.04)
Bouteloua rigidiseta°	0.41 (0.04)	0.52 (0.03)	0.14 (0.02)	0.20 (0.03)
Cenchrus ciliaris°	0.49 (0.07)	0.59 (0.06)	0.08 (0.02)	0.14 (0.02)
Chloris pluriflora	0.39 (0.03)	0.50 (0.02)	0.15 (0.04)	0.27 (0.03)
Erioneuron pilsoum°	0.43 (0.02)	0.49 (0.04)	0.18 (0.03)	0.29 (0.03)
Hilaria belangeri°	0.34 (0.04)	0.56 (0.02)	0.12 (0.02)	0.20 (0.04)
Schizachyrium scoparium	0.44 (0.01)	0.51 (0.02)	0.24 (0.04)	0.30 (0.03)
Sorghastrum nutans°	0.46 (0.02)	0.54 (0.04)	0.20 (0.05)	0.23 (0.03)
Stipa leucotricha (C3)	0.35 (0.03)	0.57 (0.05)	0.11 (0.04)	0.18 (0.03)
Tripsacum dactyloides	0.30 (0.02)	0.50 (0.01)	0.06 (0.01)	0.17 (0.02)
All standing litter (n=105)	0.42 (0.08)	0.53 (0.05)	0.13 (0.07)	0.21 (0.07)

[a] Means are given with standard deviations in parentheses. n=10 per species unless an asterisk (°) indicates n=5.
[b] C3=grass with C_3 physiology. Species without notation have C_4 physiology.

provement over the AVHRR for canopy BRDF inversions, but its angular resolution (nine view angles per pass) will sharply enhance the use off-nadir measurements for BRDF methods.

The PCA relationships applied in Eq. (8) can be analogously applied for MISR using the eigenvector weights in Table 7c to effectively reduce the number of free leaf optical parameters. A more general representation of Eq. (8) enables the PCA approach to use any number of sensor-convolved spectral bands:

$$\rho_a = \frac{e_b}{e_a}\rho_b + \left(\overline{\rho_a} - \frac{e_b}{e_a}\overline{\rho_b}\right), \quad (9)$$

where ρ_a and ρ_b are reflectances of any two leaf optical parameters, $\overline{\rho_a}$ and $\overline{\rho_b}$ are the mean reflectance values of the entire data set in a given MISR band (Table 7a), and

Table 7. A) Mean (±1 s.d.) Green Leaf (Woody Plant+Grass) Reflectance (R) and Transmittance (T) Values in MISR Channels 1–4[a]; B) Correlation Values between Green Leaf Reflectance and Transmittance Properties; C) PCA of All Leaf Data in MISR Channels

	Channels							
	1*R*	2*R*	3*R*	4*R*	1*T*	2*T*	3*T*	4*T*
A. Mean (±1 s.d.) Refl. and Trans.								
	0.06 (0.01)	0.12 (0.02)	0.06 (0.01)	0.45 (0.05)	0.01 (0.01)	0.09 (0.04)	0.03 (0.01)	0.41 (0.06)
B. Correlation Matrix[b]								
1*R*	—	0.37°°	**0.64**	−0.11	−0.23°	−0.01	−0.16	0.04
2*R*		—	**−0.67**°°	−0.21°	0.11	0.34°°	0.20	0.16
3*R*			—	0.04	−0.24°	−0.11	−0.19	−0.21°
4*R*				—	**−0.68**°°	**−0.74**°°	**−0.67**°°	**−0.72**°°
1*T*					—	**−0.75**°°	**0.88**°°	**0.65**°°
2*T*						—	**0.92**°°	**0.92**°°
3*T*							—	**0.82**°°
4*T*								—
C. Principal Components Analysis								
Eigenvalue	*Eigenvectors*							
PC1: 0.99	−0.083	−0.169	−0.099	−0.706	−0.013	−0.142	−0.052	−0.658
PC2: 0.01	0.014	−0.020	0.026	0.624	−0.071	−0.516	−0.218	−0.540

[a] Channel numbers correspond to the band centers and widths listed in Table 2.
[b] Pearson Product Moment Method.
° P<0.05, °° P<0.0001.

Table 8. A) Mean (±1 s.d.) Grass Litter Reflectance (R) and Transmittance (T) Values in MISR Channels 1–4; B) Correlation Values between Litter Reflectance and Transmittance Properties; C) PCA of Litter Data in MISR Channels

	Channels							
	1R	2R	3R	4R	1T	2T	3T	4T
A. Mean (±1 s.d.) Refl. and Trans.								
	0.18 (0.04)	0.33 (0.08)	0.45 (0.07)	0.55 (0.05)	0.03 (0.02)	0.08 (0.05)	0.15 (0.07)	0.22 (0.07)
B. Correlation Matrix[b]								
1R	—	**0.86****	**0.75****	0.14	0.50	**0.66***	**0.66***	0.32
2R		—	**0.94****	**0.53***	0.34	**0.50***	0.36	−0.08
3R			—	**0.73****	0.15	0.27	0.17	−0.26
4R				—	−0.24	−0.25	−0.42	**−0.72****
1T					—	**0.93****	**0.84****	**0.68****
2T						—	**0.92****	**0.71***
3T							—	**0.90****
4T								—
C. Principal Components Analysis								
Eigenvalue	*Eigenvectors*							
PC1: 0.98	−0.209	−0.391	−0.532	−0.640	−0.036	−0.096	−0.179	−0.259
PC2: 0.02	0.102	0.023	−0.154	−0.355	0.290	0.468	0.547	0.486

[a] Channel numbers correspond to the band centers and widths listed in Table 2.
[b] Pearson Product Moment Method.
* $P<0.05$, ** $P<0.0001$.

e_a *and* e_b are the eigenvector weights of the first principal component corresponding to the leaf parameters (Table 7c). Similar equations can be written for transmittance parameters as shown in Eq. (8). From these analyses, it appears that four free leaf optical parameters (assuming MISR Channels 2 and 4 are used) can be reduced to one free NIR Channel (4) reflectance variable. All others can be constrained or linked in a similar manner to the AVHRR channels using the PCA weightings in Table 7c.

Correlation analyses of the litter spectra demonstrated shifts in MISR band relationships from those found using the green leaf spectral data (Table 8). Most of the correlations among transmittance parameters persisted as did the Band 1/3 and 2/3 relationships. Several of the Band 4 (NIR) reflectance correlations with Bands 1–3 transmittance were eliminated, while others between Bands 1–2 reflectance and Bands 2–3 transmittance emerged. The first principal component accounted for 98% of the total variance. All reflectance (Channels 1–4) and two of the transmittance (Channels 3–4) bands contributed significantly to PC 1. As with AVHRR-convolved leaf spectra, changes in leaf optical properties associated with canopy senescence could adversely influence LAI retrievals if constraints and linkages determined for green leaf parameters are used in BRDF inversions. Again, this suggests the use of the green leaf optical correlations found in Table 7 (e.g., Channel 4 refl. vs. Channel 1–3 trans.) in a BRDF inversion to detect the onset of leaf senescence.

With the MODIS instrument, two to three additional and sufficiently unique channels are available beyond those provided by MISR for use in canopy BRDF inversions. These channels (5–7) are centered at 1240 nm, 1640 nm, and 2130 nm (Table 2). The correlation and principal components analyses for leaf and litter spectra convolved to MODIS Channels 1–7 are summarized in Tables 9 and 10. Many of the previously described relationships from the AVHRR and MISR channels apply to MODIS. Among green leaf spectra, the three additional SWIR channels were correlated, although only Band 5/6 and Band 6/7 surpassed our threshold correlation value of ±0.50, $p<0.05$. Channel 5 was highly correlated with all transmittance measurements, but poorly correlated with Channel 7 reflectance. Although Band 6 and 7 reflectances were highly correlated, their correlations with reflectance and transmittance measurements in most other channels were poor.

Principal components analysis demonstrated that Bands 5–7 played a significant role in producing the first PC for both green leaf (PC1=99%; Table 9c) and litter (PC1=97%; Table 10c) spectra. This finding, when combined with the correlation results, indicates these SWIR channels are generally sensitive to shifts from green to senescent leaf material. Therefore, a combination of these channels may be useful in adding observational information for canopy BRDF model inversions that is unique from the AVHRR and MISR optical channels. The number of free MODIS leaf optical parameters that might be linked or constrained in an inversion depends upon the number of channels used, and thus will not be suggested here. Using Eq. (9), any number of parameters

Table 9. A) Mean (±1 s.d.) Green Leaf (Woody Plant+Grass) Reflectance (*R*) and Transmittance (*T*) Values in MODIS Channels 1–7; B) Correlation Values between Green Leaf Reflectance and Transmittance Properties; C) PCA of All Leaf Data in MODIS Optical Channels 1–7

	Channels													
	1*R*	2*R*	3*R*	4*R*	5*R*	6*R*	7*R*	1*T*	2*T*	3*T*	4*T*	5*T*	6*T*	7*T*
A. Mean (±1 s.d.) Refl. and Trans.														
	0.07 (0.01)	0.45 (0.05)	0.06 (0.01)	0.11 (0.02)	0.42 (0.04)	0.31 (0.04)	0.16 (0.04)	0.03 (0.01)	0.41 (0.06)	0.01 (0.00)	0.09 (0.04)	0.42 (0.04)	0.34 (0.06)	0.20 (0.07)
B. Correlation Matrix[b]														
1*R*	—	0.07	**0.75****	**0.71****	−0.11	−0.24*	−0.23*	−0.11	−0.19	−0.13	−0.08	−0.11	−0.20	−0.16
2*R*		—	−0.12	−0.23*	**0.97****	**0.58****	0.19	**−0.70****	**−0.72****	**−0.68****	**−0.74****	**0.97****	**−0.71****	**−0.69****
3*R*			—	0.46**	−0.19	−0.28*	−0.25*	−0.14	0.01	−0.18	−0.03	−0.19	−0.02	0.01
4*R*				—	−0.24*	−0.08	0.03	0.25*	0.17	0.18	0.34*	−0.24*	0.21*	0.24*
5*R*					—	**0.73****	0.38**	**−0.72****	**−0.71****	**−0.72****	**−0.72****	**0.99****	**−0.62****	**−0.59****
6*R*						—	**0.90****	−0.44**	−0.26*	**−0.54****	−0.28	**0.73****	0.01	0.06
7*R*							—	−0.15	0.08	−0.26*	0.06	0.38**	0.38**	0.44**
1*T*								—	**0.83****	**0.94****	**0.93****	**−0.72****	**0.69****	**0.63****
2*T*									—	**0.73****	**0.93****	**−0.71****	**0.92****	**0.87****
3*T*										—	**0.83****	**−0.72****	**0.54****	**0.50****
4*T*											—	**−0.72****	**0.85****	**0.82****
5*T*												—	**−0.63****	**−0.59****
6*T*													—	**0.99****
7*T*														—
C. Principal Components Analysis														
Eigenvalue	*Eigenvectors*													
PC1: 0.99	−0.063	−0.440	−0.056	−0.108	−0.415	−0.312	−0.163	−0.033	−0.400	−0.013	−0.083	−0.415	−0.332	−0.201
PC2: 0.01	0.024	0.320	0.018	0.011	0.302	0.113	−0.031	−0.124	−0.336	−0.051	−0.271	0.302	−0.482	−0.514

[a] Channel numbers correspond to the band centers and widths listed in Table 2.
[b] Pearson Product Moment Method.
* $P<0.05$, ** $P<0.0001$.

Table 10. A) Mean (±1 s.d.) Grass Litter Reflectance (R) and Transmittance (T) Values in MODIS Channels 1–7; B) Correlation Values between Litter Reflectance and Transmittance Properties; C) PCA of All Litter Data in MODIS Optical Channels 1–7

	Channels													
	1*R*	2*R*	3*R*	4*R*	5*R*	6*R*	7*R*	1*T*	2*T*	3*T*	4*T*	5*T*	6*T*	7*T*
A. Mean (±1 s.d.) Refl. and Trans.														
	0.44 (0.08)	0.55 (0.05)	0.22 (0.05)	0.33 (0.08)	0.57 (0.06)	0.53 (0.08)	0.42 (0.11)	0.14 (0.07)	0.22 (0.07)	0.04 (0.02)	0.08 (0.04)	0.57 (0.06)	0.23 (0.08)	0.16 (0.09)
B. Correlation Matrix[b]														
1*R*	—	**0.69***	**0.92****	**0.97****	0.07	−0.19	−0.40	0.27	−0.19	0.28	0.36	0.07	**−0.78****	**−0.82****
2*R*		—	0.40	**0.54***	**0.75***	0.46	0.16	−0.38	**−0.71***	−0.22	−0.24	**0.75****	**−0.85****	**−0.77****
3*R*			—	**0.97****	−0.22	−0.42	**−0.57***	**−0.51***	0.08	0.49	**0.58***	−0.22	**−0.57***	**−0.66***
4*R*				—	−0.07	−0.34	**−0.54***	0.39	−0.08	0.41	**0.50***	−0.08	**−0.72***	**−0.79****
5*R*					—	**0.89****	**0.70***	**−0.84****	**−0.89****	**−0.64***	**−0.72***	**0.99****	−0.47	−0.29
6*R*						—	**0.93****	**−0.91****	**−0.79****	**−0.82****	**−0.90****	**0.89****	−0.13	0.08
7*R*							—	**−0.83****	**−0.57***	**−0.84****	**−0.91****	**0.68***	0.18	0.38
1*T*								—	**0.87****	**0.90****	**0.95****	**−0.84****	0.20	0.01
2*T*									—	**0.69***	**0.72***	**−0.89****	**0.64***	0.47
3*T*										—	**0.97****	**−0.64***	0.04	−0.14
4*T*											—	**−0.72****	0.01	−0.19
5*T*												—	−0.47	−0.29
6*T*													—	**0.97****
7*T*														—
C. Principal Components Analysis														
Eigenvalue	*Eigenvectors*													
PC1: 0.97	−0.317	−0.396	−0.161	−0.241	−0.412	−0.384	−0.305	−0.100	−0.158	−0.028	−0.057	−0.412	−0.162	−0.114
PC2: 0.02	0.340	0.099	0.248	0.386	−0.085	−0.261	−0.466	0.327	0.176	0.209	0.313	−0.085	−0.137	−0.259

[a] Channel number correspond to the band centers and widths listed in Table 2.
[b] Pearson Product Moment Method.
* $P<0.05$, ** $P<0.0001$.

can be considered for linkage depending on the application and canopy type (e.g., live vs. senescent canopies).

CONCLUSIONS

Recent advances in BRDF model inversion techniques have demonstrated the potential utility in using an inherent sensor attribute—angular resolution—to quantify the structural and biophysical attributes of vegetation (Gerstl, 1990; Liang and Strahler, 1993; Privette et al., 1994; Braswell et al., 1996; Privette et al., 1996). At the same time, these studies have established the need for improved angular, spectral, and spatial resolution of off-nadir viewing instruments for vegetation remote sensing (e.g., Asner et al., 1997). In addition, the need for simplification of canopy BRDF models and BRDF model inversion techniques has been highlighted.

Using a large leaf optical properties data set representing a diverse array of grass species and woody plant growthforms, we showed that species within each vegetation type have similar leaf reflectance characteristics in the visible spectral region. However, visible-range reflectance differed significantly between the woody plant and grass groups. Both green leaves and litter were more variable in the NIR and SWIR regions of the spectrum. Once convolved to AVHRR spectral response functions, leaf optical properties were successfully constrained and linked using correlation, regression, and principal components analyses. The significant differences in AVHRR-convolved green leaf and litter optical properties and interrelationships may provide a radiometrically sensitive means to detect the onset of canopy senescence that occurs due to climatic (e.g., drought) events and phenological change. These results also highlight the problems inherent in using one set of constraints and relationships in BRDF inversions on live and standing dead leaf canopies.

Both MODIS and MISR sensors, with increased spectral, angular, and spatial resolution over the AVHRR, will play a major role in future developments of canopy BRDF inversion approaches to vegetation remote sensing. Because of the strong correlations between visible bands, MISR provides similar spectral information to the AVHRR when applied to BRDF inversions. However, the significantly increased angular resolution of MISR will provide an unprecedented opportunity to utilize BRDF model inversion methods. With three shortwave IR channels, MODIS will provide two to three sufficiently unique optical channels for BRDF inversions. The synergism of MODIS and MISR will provide high quality angular data to estimate vegetation canopy attributes from space.

The leaves used in this study were collected from a wide variety of species with contrasting morphology, roughness, and physiology, and from spatially heterogeneous ecosystems along a broad climate gradient. The interrelationships found in this study should therefore be applicable to many woodlands, savannas, shrublands, and grasslands. The equations presented for the AVHRR leaf optical properties are ready for use in current BRDF model inversion efforts in ecosystems containing the species studied here. The PCA weighting results for MODIS and MISR channels are also ready for use in Eq. (9) to reduce the number of leaf optical parameters when these instruments become available for BRDF inverse modeling studies. We feel these relationships will allow the ratio of unique observations to free model parameters to increase in a physically robust manner. Our current efforts are centered on applying these findings to BRDF inversions over these biomes. Beyond the vegetation types represented in this study, it is unclear how broadly applicable these relationships will be, and thus, we are currently acquiring leaf optical characteristics in other biomes.

We sincerely thank Sam Fuhlendorf, Alan Townsend, and Steven Zitzer for assistance in collecting leaf and litter samples. Ann Bateson provided excellent comments and suggestions. G. P. A. especially appreciates the help and warm reception provided by ranchers, cowboys, and friends along the Texas savanna–woodland transect. This work was supported by NASA Innovative Research Grant NAGW-4689, NASA EOS Interdisciplinary Science Award NAGW-2662, and a NASA Earth Systems Science Fellowship Award to G. P. A. The National Center for Atmospheric Research is sponsored by the National Science Foundation.

REFERENCES

Amos, B. B., and Gehlback, F. R. (1988), *Edwards Plateau Vegetation*, Baylor University Press, Waco, TX.

Archer, S. (1995), Tree-grass dynamics in a Prosopis-thornscrub savanna parkland: reconstructing the past and predicting the future. *Ecoscience* 2:83–99.

Ardanuy, P. E., Han, D., and Salomonson, V. V. (1991), The moderate resolution imaging spectrometer (MODIS) and data system requirements. *IEEE Trans. Geosci. Remote Sens.* 29:75–87.

Asner, G. P., Braswell, B. H., Schimel, D. S., and Wessman, C. A. (1998), Ecological research needs from multi-angle remotely sensed data. *Remote Sens. Environ.* 63:155–165.

Asner, G. P., Wessman, C. A., and Privette, J. L. (1997), Unmixing the directional reflectances of AVHRR sub-pixel landcovers. *IEEE Trans. Geosci. Remote Sens.* 35:868–878.

Barnsley, M. J., Strahler, A. H., Morris, K. P., and Muller, J.-P. (1994), Sampling the surface bidirectional reflectance distribution function: 1. Evaluation of current and future satellite sensors. *Remote Sens. Rev.* 8:271–311.

Braswell, B. H., Schimel, D. S., Privette, J. L., et al. (1996), Extracting ecological and biophysical information from AVHRR optical data: an integrated algorithm based on inverse modeling. *J. Geophys. Res.* 101:23,335–23,345.

Daughtry, C. S. T., Ranson, K. J., and Biehl, L. L. (1989), A new technique to measure the spectral properties of conifer needles. *Remote Sens. Environ.* 27:81–91.

Fetcher, N., Oberbauer, S. F., and Chazdon, R. L. (1994),

Physiological ecology of plants. In *La Selva: Ecology and Natural History of a Neotropical Rain Forest* (L. McDade, K. S. Bawa, H. Hespenheide, and G. S. Hartshorn, Eds.), University of Chicago Press, Chicago, pp. 128–141.

Field, C. B., Randerson, J. T., and Malmstrom, C. M. (1995), Global net primary production: combining ecology and remote sensing. *Remote Sens. Environ.* 51:74–88.

Fourty, Th., Baret, F., Jacquemoud, S., Schmuck, G., and Verdebout, J. (1996), Leaf optical properties with explicit description of its biochemical composition: direct and inverse problems. *Remote Sens. Environ.* 56:104–117.

Gao, B.-C., and Goetz, A. F. H. (1995), Retrieval of equivalent water thickness and information related to biochemical components of vegetation canopies from AVIRIS data. *Remote Sens. Environ.* 52:155–162.

Gates, D. M., Keegan, H. J., Schleter, J. C., and Wiedner, V. R. (1965), Spectral properties of plants. *Appl. Opt.* 4:11–20.

Goel, N. S. (1988), Models of vegetation canopy reflectance and their use in estimation of biophysical parameters from reflectance data. *Remote Sens. Rev.* 4:1–212.

Goel, N. S., and Thompson, R. L. (1984), Inversion of canopy reflectance models for estimating agronomic variables. V. Estimation of leaf area index and average leaf angle using measured canopy reflectances. *Remote Sens. Environ.* 16: 69–85.

Gerstl, S. A. W. (1990), Physics concepts of optical and radar reflectance signatures: a summary review. *Int. J. Remote Sens.* 11:1109–1117.

Hatch, S. L., Gandhi, K. N., and Brown, L. E. (1990), Checklist of the vascular plants of Texas, Texas Agricultural Experiment Station, Texas A&M University, College Station.

Heitschmidt, R. K., Schultz, R. D., and Scifres, C. J. (1986), Herbaceous biomass dynamics and net primary production following chemical control of honey mesquite. *J. Range Manage.* 39:67–71.

Jacquemoud, S., Baret, F., and Hanocq, J. F. (1992), Modeling spectral and bidirectional soil reflectance. *Remote Sens. Environ.* 41:123–132.

Jacquemoud, S., Ustin, S. L., Verdebout, J., Schmuck, G., Andreoli, G., and Hosgood, B. (1996), Estimating leaf biochemistry using the PROSPECT leaf optical properties model. *Remote Sens. Environ.* 56:194–202.

Lee, D. W., and Graham, R. (1986), Leaf optical properties of rainforest sun and extreme shade plants. *Am. J. Bot.* 73: 1100–1108.

Li, X., Strahler, A. H., and Woodcock, C. E. (1995), A hybrid geometric optical-radiative transfer approach for modeling albedo and directional reflectance of discontinuous canopies. *IEEE Trans. Geosci. Remote Sens.* 33:466–480.

Liang, S., and Strahler, A. H. (1993), An analytic BRDF model of canopy radiative transfer and its inversion. *IEEE Trans. Geosci. Remote Sens.* 31:1081–1095.

Marshak, A. L. (1989), The effect of the hot spot on the transport equation in plant canopies. *J. Quant. Spectrosc. Radiat. Trans.* 42:615–630.

McMahan, C. A., Frye, R. G., and Brown, K. L. (1984), *The Vegetation Types of Texas*, Texas Parks and Wildlife Department, Austin.

Mesarch, M. A., Walter-Shea, E. A., Middleton, S. A., Chan, S. A., and Asner, G. P. (in review), A revised methodology for conifer needle spectral optical properties. *Remote Sens. Environ.*

Middleton, E. M., Chan, S. S., Mesarch, M. A., and Walter-Shea, E. A. (1996), A revised methodology for spectral optical properties of conifer needles. *IGARSS'96 Dig.* 2:1005–1009.

Myneni, R. B., Gutschick, V. P., Asrar, G., and Kanemasu, E. T. (1988), Photon transport in vegetation canopies with anisotropic scattering. *Agric. For. Meteorol.* 42:1–40.

Myneni, R. B., and Asrar, G. (1993), Radiative transfer in three-dimensional atmosphere–vegetation media. *J. Quant. Spectrosc. Radiat. Trans.* 49:585–598.

Myneni, R. B., Ross, J., and Asrar, G. (1989), A review on the theory of photon transport in leaf canopies. *Agric. For. Meterol.* 45:1–153.

Poorter, L., Oberbauer, S. F., and Clark, D. B. (1995), Leaf optical properties along a vertical gradient in a tropical rain forest canopy in Costa Rica. *Am. J. Bot.* 82:1257–1263.

Privette, J. L., Emery, W. J., and Schimel, D. S. (1996), Inversion of a vegetation reflectance model with NOAA AVHRR data. *Remote Sens. Environ.* 58:187–200.

Privette, J. L., Myneni, R. B., Tucker, C. J., and Emery, W. J. (1994), Invertibility of a 1-D discrete ordinates canopy reflectance model. *Remote Sens. Environ.* 48:89–105

Privette, J. L., Myneni, R. B., Emery, W. J., and Hall, F. G. (1996), Optimal sampling conditions for estimating grassland parameters via reflectance model inversions. *IEEE Trans. Geosci. Remote Sens.* 34:272–284.

Ross, J. K. (1981), *The Radiation Regime and Architecture of Plant Stands,* Kluwer Boston, Hingham, MA.

Running, S. W., Justice, C. O., Salomonson, V., et al. (1994), Terrestrial remote sensing science and algorithms planned for EOS/MODIS. *Int. J. Remote Sens.* 15:3587–3620.

Running, S. W., Loveland, T. R., and Pierce, L. L. (1994), A vegetation classification logic based on remote sensing for use in global biogeochemical models. *Ambio* 23:77–89.

Shultis, J. K., and Myneni, R. B. (1988), Radiative transfer in vegetation canopies with anisotropic scattering. *J. Quant. Spectrosc. Radiat. Trans.* 39:115–129.

Thomas, J. R., Namken, L. M., Oerther, G. F., and Brown, R. G. (1971), Estimating leaf water content by reflectance measurements. *Agron. J.* 63:845–847.

Verdebout, J., Jacquemoud, S. and Schmuck, G. (1994), Optical properties of leaves: modelling and experimental studies. In *Imaging Spectrometry—A Tool for Environmental Observations* (J. Hill and J. Megier, Eds.), ECSC, EEC, EAEC, Brussels and Luxembourg, pp. 169–191.

Walter-Shea, E. A., and Norman, J. M. (1991), Leaf optical properties. In *Photon–Vegetation Interactions* (R. B. Myneni and J. Ross, Eds.), Springer-Verlag, Berlin, pp. 229–251.

Wessman, C. A., Aber, J. D., Peterson, D. L., and Melillo, J. M. (1988), Remote sensing of canopy chemistry and nitrogen cycling in temperate forest ecosystems, *Nature* 335: 154–156.

Wessman, C. A., and Asner, G. P. (in press), Ecosystems and the problems of large-scale measurements. In *Successes, Limitations, and Frontiers in Ecosystem Ecology* (P. Groffman and M. Pace, Eds.), Springer-Verlag, Berlin.

Wooley, J. T. (1971), Reflectance and transmittance of light by leaves. *Plant Physiol.* 47:656–662.